

PAPER • OPEN ACCESS

Effect of trailing edge thickness on the performance of a helium turboexpander used in cryogenic refrigeration and liquefaction cycles

To cite this article: Ashish Alex Sam and Parthasarathi Ghosh 2017 *IOP Conf. Ser.: Mater. Sci. Eng.* 171 012021

View the [article online](#) for updates and enhancements.

Related content

- [Parametric studies on floating pad journal bearing for high speed cryogenic turboexpanders](#)
A Jain, M M Jadhav, S Karimulla et al.
- [Thermodynamic analysis and economical evaluation of two 310-80 K pre-cooling stage configurations for helium refrigeration and liquefaction cycle](#)
Z G Zhu, M Zhuang, Q F Jiang et al.
- [Helium refrigeration system for hydrogen liquefaction applications](#)
J Kumar, SR Nair, RS Menon et al.



ECS **240th ECS Meeting**
Oct 10-14, 2021, Orlando, Florida

Register early and save up to 20% on registration costs

Early registration deadline Sep 13

REGISTER NOW

Effect of trailing edge thickness on the performance of a helium turboexpander used in cryogenic refrigeration and liquefaction cycles

Ashish Alex Sam*, Parthasarathi Ghosh

Cryogenic Engineering Centre, Indian Institute of Technology Kharagpur, India - 721302

E-mail: ashishalexsam@gmail.com

Abstract. Turboexpanders in cryogenic refrigeration and liquefaction cycles, which is of radial inflow configuration, constitute stationary and rotating components like nozzle, a rotating wheel and a diffuser. The relative motion between the stationary and rotating components and the interactions of secondary flows and vortices at different stages make the turboexpander flow unsteady. Computational Fluid Dynamics (CFD) analysis of this flow is essential to identify the scope for improvement in efficiency. The trailing edge vortex formed due to the mixing of the pressure and suction side streams is an important phenomenon to analyse, as this leads to efficiency degradation of the machine. Additionally, there are mechanical vibrations and dynamic loading associated with. This flow non-uniformity at the exit should be suppressed as this may affect the pressure recovery process in the diffuser and thereby the turboexpander's performance. The strength of this vortex depends upon the geometrical parameters like trailing edge shape, thickness etc. In this paper, transient CFD analyses of a cryogenic turboexpander designed for helium refrigeration and liquefaction cycles using Ansys CFX[®] were performed to investigate the effect of trailing edge thickness on the turboexpander performance and the performance characteristics and the flow patterns were compared to understand the flow characteristics in each case.

1. Introduction

The flow within a cryogenic turboexpander is highly complex due to its three dimensional, viscous, turbulent and unsteady natures. These complex flow characteristics, associated with the various flow parameters degrade the performance of the machine. In order to improve the performance of the machine, a detailed analysis of the flow field in a cryogenic turboexpander is essential for the accurate prediction of the effect of various geometric and flow parameters on the turboexpanders performance [1]. As it is impossible to capture this complex flow behaviour through experiments, computational analysis has to be employed to analyse the same.

Sam and Ghosh [2] has compared the flow field of a helium turboexpander with that of a nitrogen turboexpander using CFD and reported the trailing edge thickness as one of the major sources of losses in a cryogenic helium turboexpander. Therefore any improvement in the turboexpander design calls for an extensive analysis of the flow structures at the trailing edge for understanding the influence of trailing edge profile on the cryogenic helium turboexpanders performance.

The effect of trailing edge profile on the performance of turbomachines has been a subject of study. The loss generation mechanism associated with the trailing edge shape and thickness in axial turbines



has been discussed by Denton [3]. Zhou et al [4] has performed experimental and numerical analysis on an ultra-high lift low pressure axial turbine, to investigate the effect of trailing edge thickness on the losses and reported that the loss generation increased with increase in trailing edge thickness. Although the provision of thick trailing edges imparts sufficient strength for the blades to withstand the fluid stresses, it increases the loss generation [4]. Reduction in loss generation with thinner trailing edges was also reported by Prust and Helon [5] for an axial turbine stator through experimental analysis. Works have also been reported on the effect of trailing edge blade shape on the turbomachines performance.

Although a few publications, which focus on the effects of trailing edge shape and thickness on the performance of axial turbomachines, are available, those for radial inflow turbines and especially for cryogenic turboexpanders are scarce in the open literature.

2. Objective

In this paper, unsteady CFD analysis of a cryogenic helium turboexpander was performed to study the effect of trailing edge thickness on the performance of the turboexpander. A three dimensional transient analysis of the turboexpander was performed for three different trailing edge thicknesses. The study includes a detailed investigation of the flow behaviour at the trailing edge of the helium turboexpander and identification of the various sources of loss generation.

3. Numerical modelling

A cryogenic turboexpander developed for large scale helium refrigeration and liquefaction cycles was used for the present study. The turboexpander specifications are mentioned in table 1. The design of the turboexpander was made based on the design methodology developed by Kun and Sentz [6] with the preliminary design based on Balje's $n_s d_s$ chart [7]. The specific speed and specific diameter used for the preliminary design are given in table 1. The 3D turbine blade profile was obtained using the blade profile computation technique proposed by Hasselgruber [8]. Figure 1, shows the main components of the turboexpander along with the basic fluid flow path in a cryogenic turbine. A straight duct was provided at the turbine –wheel diffuser interface to curb the flow non-uniformity at the turbine wheel blade exit.

The 3D modelling and meshing of the turboexpander was performed using the various design and meshing modules available in the commercial software package Ansys CFX[®]. The 3D model of the cryogenic turboexpander is shown in figure 2. The turbine blade wheel profile was generated using

Table 1. Turboexpander specifications [9]

Impeller major diameter	16 mm
Design speed	264000 rpm
Rated power	1.8 kW
Total pressure at inlet	16.5 bar
Total temperature at inlet	70 K
Mass flow rate	0.05 kg/s
Static pressure at exit	11 bar
Number of stator blades	17
Number of rotor blades	13
Specific speed	0.587
Specific diameter	3.14

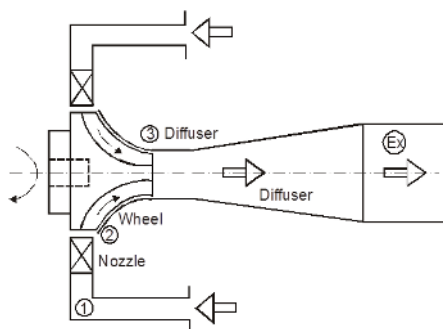


Figure 1. Fluid flow path in a turbine [10]

State points:
 1: Inlet to nozzle
 (overall inlet)
 2: Inlet to wheel
 (exit from nozzle)
 3: Inlet to diffuser
 (exit from wheel)
 Ex: Exit from diffuser
 (overall exit)

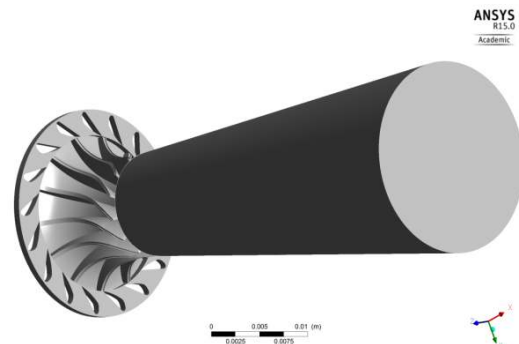


Figure 2. 3D model of turboexpander

ANSYS BladeGen[®] and the ANSYS TurboGrid[®] was used to obtain the mesh. The details of the mesh in various components are given in table 2. In order to capture the trailing edge flow structures, an H type topology were used at the trailing edges and the Y + value was maintained around 1 at the blade and end walls to resolve the boundary layer effects. A grid convergence test was performed to finalize the minimum number of mesh nodes required for accurate prediction of the turboexpander performance. As the number of mesh elements and its distribution influence the computational results, a grid independence test was performed to evaluate its impact (figure 3). As seen in the figure, the efficiency increases with increase in the number of nodes and this rise becomes less significant beyond 14.5 million nodes. In the present case the total number of nodes was chose to be around 14.5 million as a further increase in the total number of nodes would result in longer computational time.

The SST k- ω turbulence model with an automatic wall treatment was used for the present computational analysis [11]. The SST k- ω model provided good prediction of the trailing edge effects of an ultra-high lift low pressure turbine [4]. As the flow at the trailing edge is dominated by unsteady effects, the rotor-stator interface was modelled using the transient rotor-stator model. The time step for the current effort was selected based on a time sensitivity analysis, the details of which are reported in an earlier publication by the authors [12]. A time step of 1.5° with 5 internal coefficient loops for a convergence criterion of 10^{-3} was opted. The mass flow rate at inlet and static pressure at outlet boundary specification criteria was used for the computation. The unsteady analysis was initialised with a fully converged steady state solution. The ideal gas equation of state was used to specify the helium fluid properties [13].

Table 2. Mesh specifications for various components

Domain	Number of nodes	Method	Mesh type/ type of elements
Nozzle	7,69,033	Sweep	Unstructured, mostly hexahedral with small number of wedges
Turbine	134,71,588	H grid topology	Structured, with hexahedral elements
Diffuser	9,73,471	Patch conforming method	Unstructured, mostly hexahedral with small number of wedges

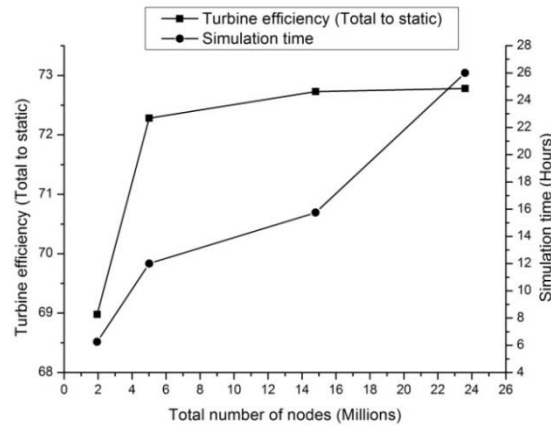


Figure 3. Grid independency test

4. Results and Discussion

The unsteady CFD analysis of the cryogenic helium turboexpander was performed for three different trailing edge thicknesses. The turbine wheel blade trailing edge was elliptic in shape. El-Gendi [14] has reported that an elliptic trailing edge provided uniform pressure distribution at the trailing edge and minimised the losses. Denton [3] found out that an elliptical shaped trailing edge provided improved performance for an axial turbine.

The trailing edge thicknesses for the three cases are presented in table 3. The trailing edge thicknesses are represented in terms of trailing edge elliptic ratio which is the ratio of major to minor axis of the elliptical profile at the trailing edge (table 3). As the turbine blade chord was kept same for all the three cases, an increase in the elliptic ratio resulted in a decrease in the trailing edge thickness. The variation in trailing edge thickness with increase in trailing edge elliptic ratio is shown in figure 4.

The performance of the turboexpander for the three different cases is compared in table 4. The total to static efficiency and the base pressure coefficient are compared. The table 4 shows that there is an improvement in the turboexpander performance with the increase of trailing edge elliptic ratio. As the trailing edge thickness is reduced from case L to S, there is an improvement of almost 0.56% in the turboexpanders efficiency. To have a better understanding of this performance behaviour, the flow characteristics and the entropy generation mechanism needs to be analysed. For this, the time averaged contours of velocity, total pressure, turbulence kinetic energy and entropy and velocity vectors were plotted.

Table 3. Trailing edge thickness

Case	Trailing edge elliptic ratio
S	8
M	2
L	0.5

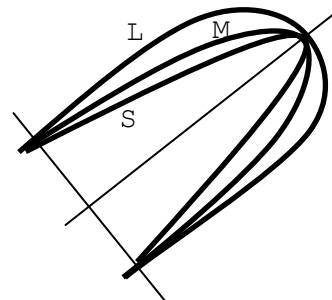


Figure 4. Trailing edge profile for the three cases

Table 4. Comparison of performance parameters

	Case S	Case M	Case L
Turbine efficiency (total to static), η_{T-st}	72.3%	72.1%	71.9%
Base pressure coefficient, C_{pb}	0.033	0.016	0.0018

The flow at the turbine wheel exit is influenced by the upstream flow characteristics. This can be seen from the velocity vectors and entropy contours in figure 5a and 5b at the mid passage of the turbine wheel. These figures clearly portray the flow structures within the turbine blade passage like the tip leakage flow, the passage vortex and the secondary flows at the end walls and blade walls, and the corresponding rise in entropy. This complex flow behaviour makes the flow at the turbine wheel exit highly non-uniform.

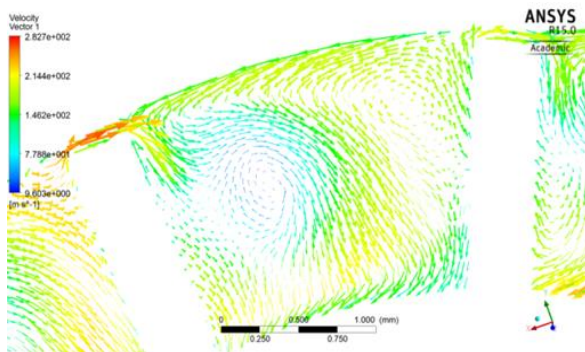


Figure 5a. Velocity vector in a constant stream wise location

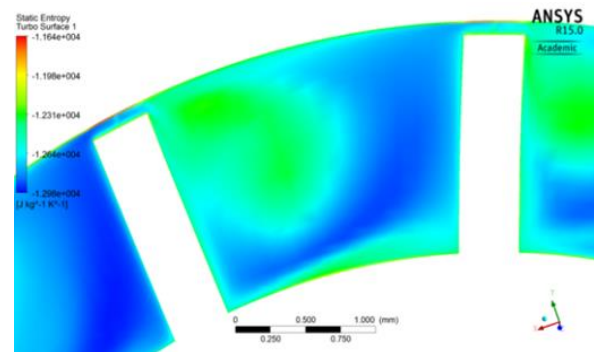


Figure 5b. Entropy contour in a constant stream wise location

Figure 6 shows the velocity vectors at the mid-span of the blade for all the three cases. The total pressure distribution, turbulent kinetic energy and the entropy contours at mid-span in the blade to blade view are shown in figures 7 -9. The velocity vectors show that the wake region at the turbine wheel blade exit is larger for the thicker blade (case L). At the downstream, the mixing out of the vortices formed as a result of the mixing of pressure side and suction side fluid streams increases entropy (figure 9). In the case of thick trailing edges, in addition to the mixing of fluid streams, the separated blade boundary layers at the trailing edge also contribute to the formation of vortices. When the vortices mix out, high rates of viscous shear occurs which is a major entropy generation mechanism [15].

Base pressure, which is the pressure just behind the blade trailing edge influences the loss generation at the trailing edge and is an important parameter for the determination of trailing edge loss [3, 4, 16]. The trailing edge base pressure will be lower for a highly non-uniform flow. In the present study, base pressure coefficient (C_{pb}) a non-dimensional representation of the base pressure is used for the analysis [4]. The base pressure coefficient at the mid-span for the three cases is compared in table 4. The variation in the base pressure coefficient value shows the effect of wakes on the base pressure (table 4). The base pressure coefficient is larger for turbine blade with minimum trailing edge thickness. With increase in trailing edge thickness the boundary layer separation will be more and more will be the vortex generated at the downstream of the trailing edge which in turn decreases the base pressure.

The turbulent kinetic energy plots in figure 8, will help to locate the regions of maximum total pressure loss due to the formation of these vortices. According to Denton [3] a higher base pressure compared to the static pressure of the downstream mixed out flow will reduce the loss. It has been observed that the thinner trailing edge provides smoother flow from the pressure side to the suction side and thus reduces the loss generation due to mixing. This also delays the boundary layer separation which in turn increases the base pressure and thus reduction in loss [3].

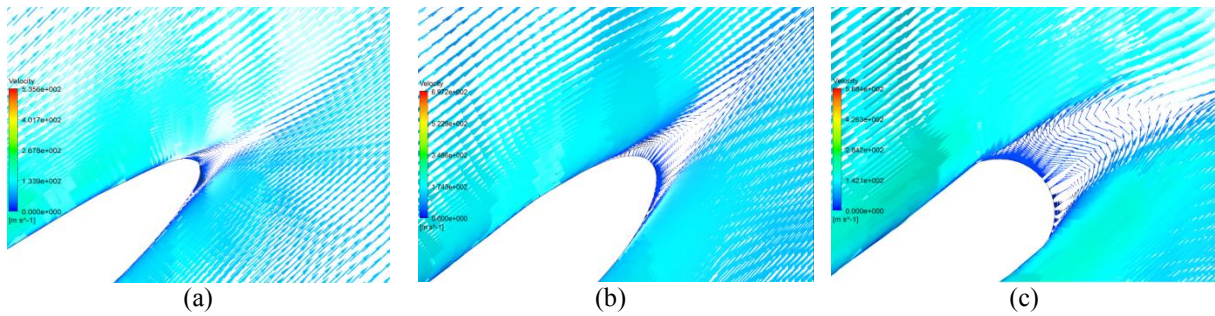


Figure 6. Velocity vector at mid-span in the blade to blade view for case (a) S (b) M (c) L

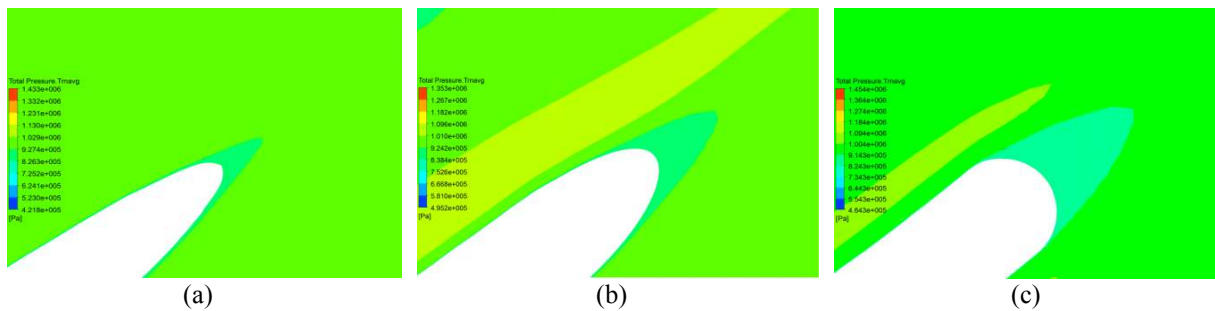


Figure 7. Total pressure contour at mid-span in the blade to blade view for case (a) S (b) M (c) L

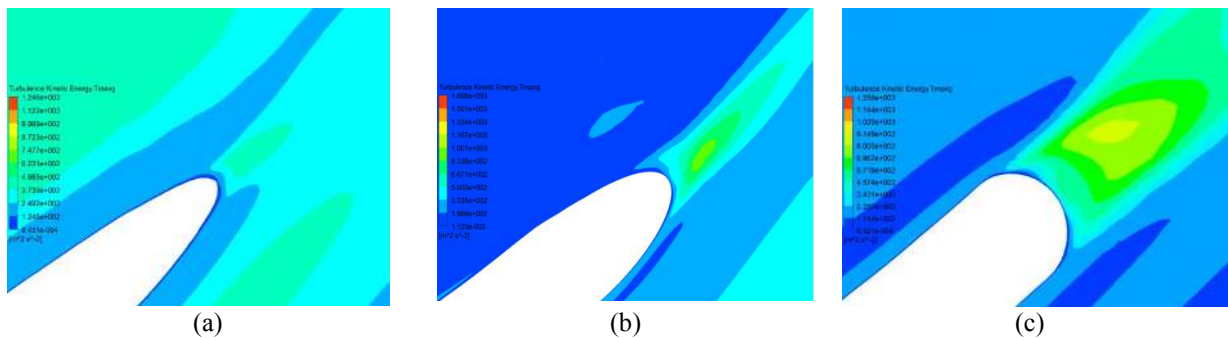


Figure 8. Turbulent kinetic energy contour at mid-span in the blade to blade view for case (a) S (b) M (c) L

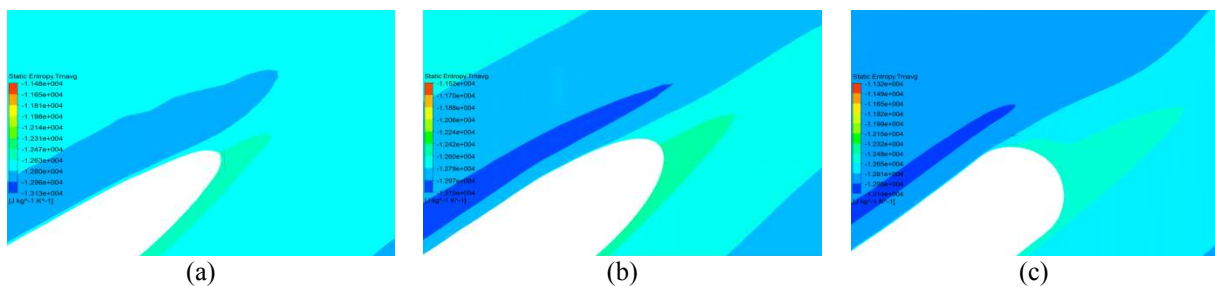


Figure 9. Entropy contour at mid-span in the blade to blade view for case (a) S (b) M (c) L

Figure 10 – 12 shows the velocity vectors in the turbine blade passage and in the straight duct in a plane cut along the axis. The plots portray the flow non-uniformity that exists at the turbine wheel exit. The mixing of different fluid streams from the various blade passages, which leads to the formation of vortices, is shown in figures 10a-12a. The presence of vortex structures is evident from these velocity vector plots. As the thickness decreases (from case L to S) the loss generation at the trailing edge is reduced, as the uniform flow at the blade exit leads to uniform distribution of the base pressure and

higher base pressure coefficient. A positive pressure gradient will accelerate the fluid layers towards the downstream, which in turn reduces the transverse velocity gradient and thereby the entropy generation. The entropy generation due to mixing of these fluid streams is depicted in Figure 10b – 12b and is lower for smaller trailing edge thickness. The flow characteristic at the turbine wheel blade also affects the flow in the straight duct, which in turn effects the flow separation in the diffuser. Therefore the trailing edge thickness in cryogenic helium turboexpander should be optimised considering the mechanical integrity and the loss generated.

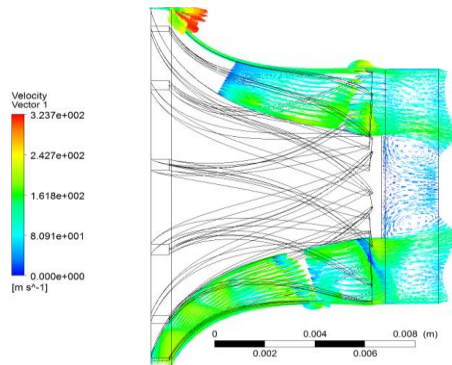


Figure 10a. Velocity vector at the turbine wheel and straight duct for case S

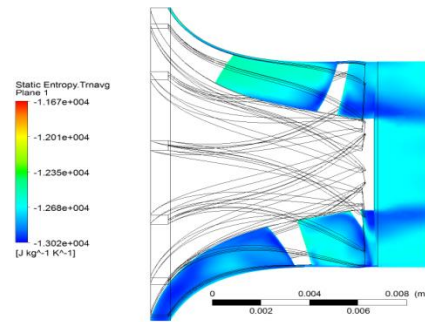


Figure 10b. Entropy contour in the turbine wheel and straight duct for case S

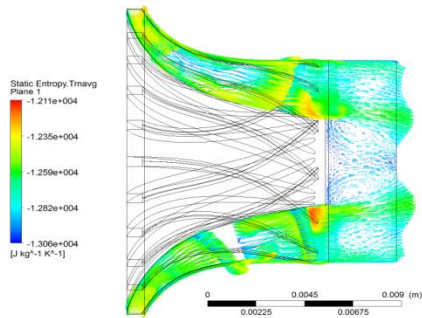


Figure 11a. Velocity vector in the turbine wheel and straight duct for case M

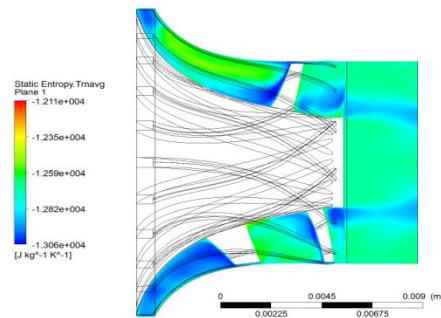


Figure 11b. Entropy contour in the turbine wheel and straight duct for case M

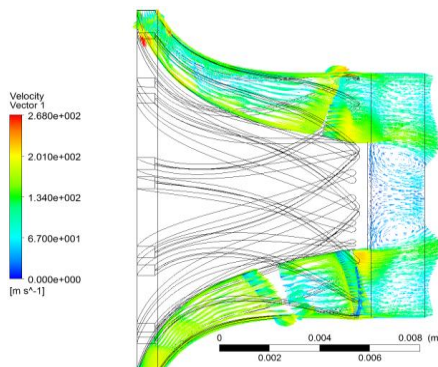


Figure 12a. Velocity vector in the turbine wheel and straight duct for case L

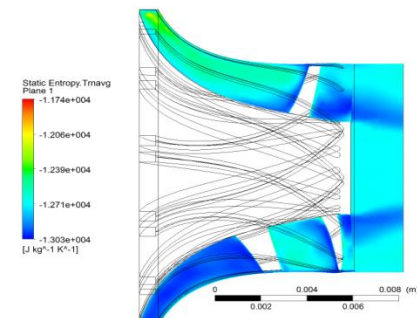


Figure 12b. Entropy contour in the turbine wheel and straight duct for case L

Conclusion

CFD analysis of the helium cryogenic turboexpander was performed for different thicknesses of the trailing edge. The performance parameters from the computational analysis for all the three cases were compared to study the influence of variation in the trailing edge thickness, on the performance of the turboexpander. The velocity vectors and contour plots of entropy, total pressure and turbulence kinetic energy helped to understand the flow characteristics and the loss generation mechanism at the trailing edge. It was observed that there was an improvement in the turboexpanders performance with the reduction in thickness. A thinner trailing edge provided smoother flow from the pressure side to suction side which reduced the entropy generation due to mixing and thus the losses. The present study along with considerations of structural integrity and machining techniques may be used to develop a design solution for the turbine wheel blade trailing edge thickness of cryogenic helium turboexpanders.

Nomenclature

\dot{m} – mass flow rate

h – enthalpy

η_{T-st} – total-to-static efficiency

$$\eta_{T-st} = \frac{h_{0,1} - h_{0,ex}}{h_{0,1} - h_{ex,s}}$$

C_{pb} – base pressure coefficient

$$C_{pb} = \frac{P_b - P_M}{P_{0,1} - P_M}$$

P_b – base pressure

P_M – mixed out static pressure, calculated at diffuser inlet

Subscripts

0 – stagnation condition

1 – inlet to the nozzle

2 – inlet to the turbine

3 – exit from the turbine wheel

ex – discharge from the diffuser

s - isentropic state

T-st – total-to-static

References

- [1] Verma R, Sam A A and Ghosh P 2015 *Phys. Procedia* **67** 373-78
- [2] Sam A A and Ghosh P 2015 *IOP Conf. Ser.: Mater. Sci. Eng.* **101** 012179
- [3] Denton J D 1993 *J. Turbomach.* **115** 621-656
- [4] Zhou C, Hodson H and Himmel C 2014 *J. Turbomach.* **136** 081011
- [5] Prust H W and Helon R M 1972 NASA technical note NASA TN D-6637, National aeronautics and space administration Washington
- [6] Kun L C and Sentz R N 1985 *Int. Conf. on Production and Purification of Coal Gas and Separation of Air* (Beijing) pp. 1-21
- [7] Balje O E 1981 *Turbomachines* (John Wiley and Sons)
- [8] Hasselgruber H 1958 Stromungsgerechte gestaltung der laufrader von radialcompressoren mit axialem laufradeintrict Konstruktion **10** (1) 22 (in German)
- [9] Chakravarty A and Singh T 2011 *Indian J. Cryogenics*, **36**(1-4) 1-9
- [10] Ghosh P 2002 *Ph.D dissertation, IIT Kharagpur*
- [11] Menter F R 2009 *Int. J. Comput. Fluid Dynamics* **23** (4) 305-16
- [12] Sam A A and Ghosh P 2016 Helium turboexpander for cryogenic refrigeration and liquefaction cycles: Transient analysis of rotor stator interaction ASME Turbo Expo (Seoul, South Korea, 13-17 June, 2016)
- [13] Thomas R J, Dutta R, Ghosh P and Chowdhury K 2012 *Cryogenics* **52**(7-9) 375–81
- [14] El-Gendi M M, Ibrahim M K, Mori K and Nakamura Y 2008 *Proc. KSAS-JSASS Joint Int. Symp. Aero. Eng.* **11** 38-42
- [15] Vagnoli S, Verstraete T, Mateos B and Sieverding C H 2015 *Proc. Inst. Mech. Eng. J. Power and Energy* **229**(5) 487 – 497
- [16] Denton J D and Xu L 1990 *J. Turbomach.* **112** 277-285